View metadata, citation and similar papers at core.ac.uk
brought to you by CORE
provided by The University of Utah: J. Willard Marriott Digital Library

Proceedings of the 28th IEEE
EMBS Annual International Conference
New York City, USA, Aug 30-Sept 3, 2006

Model-Based Image Reconstruction for Dynamic Cardiac Perfusion MRI from Sparse Data

Suyash P. Awate
School of Computing
University of Utah
UT 84112
suyash@cs.utah.edu

Edward V. R. DiBella
Department of Radiology
University of Utah
UT 84108
ed@ucair.med.utah.edu

Tolga Tasdizen
School of Computing
University of Utah
UT 84112
tolga@cs.utah.edu

Ross T. Whitaker
School of Computing
University of Utah
UT 84112
whitaker@cs.utah.edu

***Abstract*— The paper presents a novel approach for dynamic magnetic resonance imaging (MRI) cardiac perfusion image reconstruction from sparse k-space data. It formulates the reconstruction problem in an inverse-methods setting. Relevant prior information is incorporated via a parametric model for the perfusion process. This wealth of prior information empowers the proposed method to give high-quality reconstructions from very sparse k-space data. The paper presents reconstruction results using both Cartesian and radial sampling strategies using data simulated from a real acquisition. The proposed method produces high-quality reconstructions using 14% of the k-space data. The model-based approach can potentially greatly benefit cardiac myocardial perfusion studies as well as other dynamic contrast-enhanced MRI applications including tumor imaging.**

I. INTRODUCTION

Dynamic imaging is an important and rapidly growing area in magnetic resonance imaging (MRI) with profound implications for medical diagnosis and treatment. One such application is the measurement of myocardial perfusion. Subendocardial perfusion has recently been shown to be a good indicator of ischemia [1], [2]. MRI has the potential to become a widely-used non-invasive tool for myocardial perfusion measurement. The high spatial resolution in MRI allows differentiation between subendocardial and subepicardial regions [3], which is not possible with clinical positron emission tomography or single photon emission computed tomography.

Dynamic contrast-enhanced (DCE) MRI, with gadolinium as the contrast agent, tracks the exchange of this contrast agent between the blood and the myocardial tissue. The exchange is rapid and entails sampling the kinetics of the contrast-agent distribution, typically, at every heartbeat [4]. This need for high temporal resolution severely limits the resolution, spatial coverage, and signal-to-noise ratio (SNR) of current DCE-MRI acquisitions. For a reasonable field-of-view and resolution, complete heart coverage of about 10 slices with a heartbeat rate of up to 100 beats per minute entails acquisition times of less than 50 milliseconds per slice. Accounting for the magnetization-preparation time, this translates to at most 10-25 lines of k-space for each image.

Conventional MRI reconstruction of dynamic signals applies the inverse-Fourier transform to each image individually to produce a time series of images for every slice through the heart. Even with cutting-edge multi-coil methods, it is virtually impossible to obtain clinically useful images from such sparse data by independently reconstructing the time frames. Furthermore, even if the images could be reconstructed without artifacts, the SNR would be extremely low because SNR is proportional to the square root of the number of acquired k-space lines.

An effective strategy of dealing with sparse data is to incorporate prior information in the reconstruction. We propose to introduce such prior information in the form of a *parametric model* for the perfusion process. In this way, we reduce the reconstruction task from estimating each pixel intensity over time to estimating only the parameters of the model.

The proposed model-based reconstruction method leads to significant improvements in SNR with very sparse k-space data. Moreover, the gain in SNR can be traded for fewer k-space samples. This can, in turn, lead to acquisitions with higher resolutions in space or time. The proposed method has the potential to greatly benefit myocardial perfusion studies and other DCE-MRI applications, such as tumor imaging.

II. RELATED WORK

Over the years, researchers have presented a variety of methods for increasing the acquisition speed for many dynamic-MRI applications. Typically, speedup is achieved by reducing the amount of data acquired in k-space. The ratio of the total number of k-space lines to the number of lines acquired is termed the *reduction factor*, R. Current commercial systems offer cardiac perfusion imaging sequences that incorporate multi-coil parallel imaging, e.g. SENSE [1] and GRAPPA [5], and provide $R \approx 1.6$ (24 "autocalibration" lines around the center of k-space and every other line sampling ($R = 2$) outside of the center). The TSENSE method with $R = 2$ has also recently been applied to perfusion imaging [6].

A number of methods use, implicitly or explicitly, an *a priori* model for the perfusion process over time. For instance, sliding window is a data-sharing method that implicitly assumes slow object or contrast-agent (tracer) kinetics. The sliding-window strategy lends itself to both Cartesian [7], [8] and radial reconstruction [9], [10] schemes. An extension of the sliding-window approach is to use

specific acquisition patterns to match the k-space contributions of the time-varying signals. For example, the time-resolved interpolation for contrast kinetics (TRICKS) [11], [12] and the block-regional interpolation scheme for k-space (BRISK) [13] methods acquire different portions of k-space with different temporal-sampling rates. Similarly, UNFOLD-type methods [14], [15], [16] acquire even and odd phase encodes alternately in each temporal frame. Such methods have found applications in cardiac perfusion imaging [17], cardiac cine imaging [14], as well as functional MRI [14].

Faster data acquisition is still required for myocardial perfusion MRI to increase spatial coverage, increase spatial resolution, and reduce motion artifacts. The contributions in this paper can help speedup the data-acquisition stage. The proposed approach poses the reconstruction problem as an *inverse problem*. Inverse-problem approaches have found utility in static MRI applications [19], [20]. Inverse-problem methods have been applied to cardiac imaging [21], although without any parametric models. Parameterized models encode stronger prior information and, hence, may have the ability to produce superior results.

III. A PARAMETRIC MODEL FOR CARDIAC PERFUSION IMAGES

Let us assume that we have a set of magnetic resonance (MR) images for each slice in the heart, one for each time frame $t \in \mathbb{I}$. Each image comprises a set of pixels $x \in \mathbb{I}^D$ on a D-dimensional Cartesian grid. Thus, $D = 2$ implies a slice of data at each time t. Denote the pre-contrast MR image intensity at each pixel x as $I_p(x)$. Denote the input function to the heart produced by the incoming contrast agent by $C(t)$, which is a function of the time t. Then the intensities $g(x,t)$ observed at pixel x at time t are

$$g(x,t) = I_p(x) + C(t) * \beta_1(x) \exp\left(-\frac{t-\beta_3(x)}{\beta_2(x)}\right) * H(t-\beta_3) * \exp\left(-\frac{t^2}{\beta_4^2(x)}\right) \exp\left(j\phi(x)\right), \quad (1)$$

where $*$ denotes convolution, $H(t)$ denotes the discrete Heaviside-step function, and j is the imaginary unit number. Thus, the parameter set for the model is

$$\alpha = \{I_p(x), \beta_1(x), \beta_2(x), \beta_3(x), \beta_4(x), \phi(x) : \forall x\}. \quad (2)$$

We observe that (a) $\beta_1(x)$ corresponds to perfusion and scales the input function, (b) $\beta_2(x)$ and $\beta_3(x)$ describe the rate of contrast agent washout and the time delay associated with the first exponential function, respectively, and (c) $\beta_4(x)$ describes the decay rate of the second exponential function. The convolution with the second exponential function signifies the *dispersion* of the input signal. This model implicitly assumes that the phase $\phi(x)$ in the complex-MR image remains constant over time.

IV. K-SPACE SAMPLING SCHEMES

One of the most popular techniques of sampling the k-space is to sample straight lines, along the read direction, that follow a specific pattern. For instance, UNFOLD-type methods [14], [15], [16] acquire all even and all odd phase encodes alternating over time frames. The strategies in the proposed method significantly differ from conventional ones. The first proposed sampling is similar to the approach taken by Portniaguine *et al.* [21]. Here, the idea is to acquire a fixed number of k-space lines aligned along the read direction, but with the specific lines selected randomly in each time frame. In each time frame, moreover, we take 4 lines from the center of the k-space. The idea behind this approach is to get the low-frequency components in each time frame via the central k-space lines, while making the high-frequency errors across time frames as *independent* as possible. Figure 1(a) shows such a sampling scheme for one time frame.

A number of researchers use radial acquisitions for cardiac cine imaging [16] and MR-angiography applications. Radial techniques can produce higher spatial resolution, for a given amount of scan time, as compared to Cartesian imaging [22]. Compared to Cartesian k-space sampling, undersampled radial k-space sampling results in much-reduced aliasing and some streaking [23]. Thus, the second proposed sampling strategy is to acquire a pattern of equiangular radial slices through the center of the k-space in each time frame, while rotating this acquisition pattern randomly across time frames. Figure 1(b) shows the radial sampling scheme for one time frame. Figure 2 gives an example of artifacts from k-space data sampled using the two proposed strategies. The radial k-space sampling retains more information from the imaged signal.

Reconstructions from non-Cartesian k-space sampling, such as radial sampling, entail modifications to the Cartesian parallel-imaging methods. Recall that we define the parametric model for the perfusion process on the magnitude-MR data, and not on the k-space data. Thus we need methods to

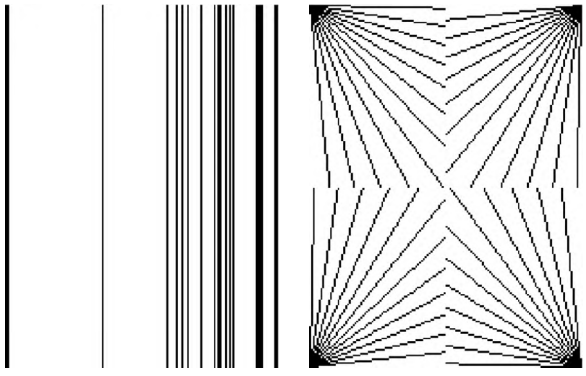

Fig. 1. Proposed k-space sampling strategies acquiring 14% k-space data. The k-space center is at the corners of the image. Black locations indicate acquired samples. (a) Sampling along the read direction: random lines in each time frame including 4 lines in each time frame passing through the k-space center. (b) Radial sampling: a pattern of equiangular radial lines through the k-space center. This pattern rotates randomly at each time frame.

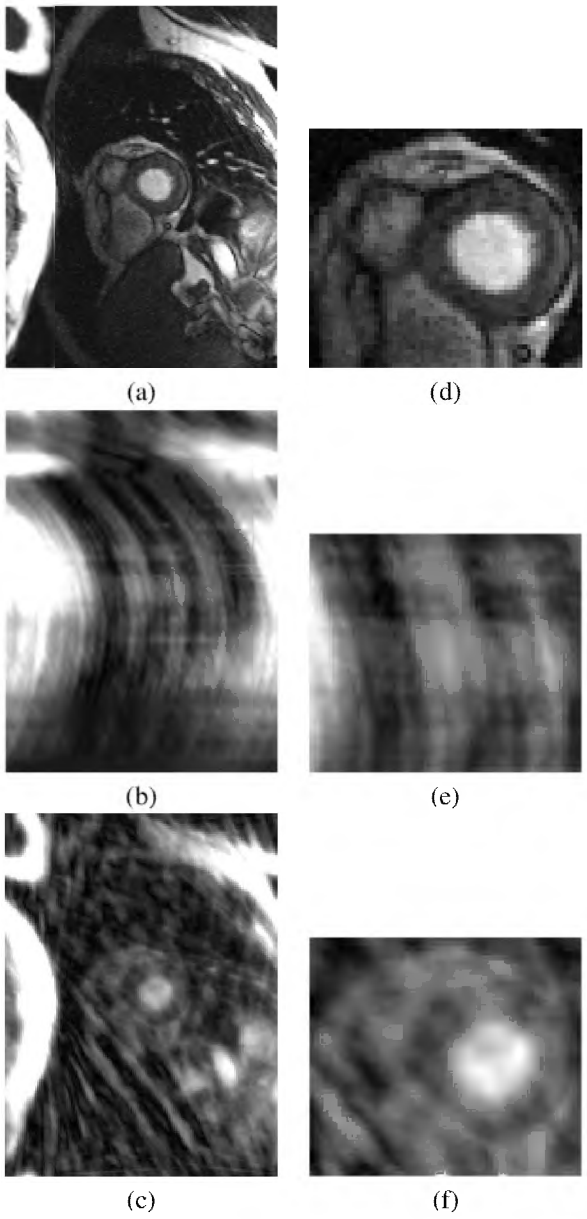

Fig. 2. (a) Magnitude of the Fourier inverse of 100% k-space data for one time frame. Magnitude of the Fourier inverse of the sparse (14%) k-space data where samples are acquired along (b) random lines (with 4 in the center each time frame) (see Figure 1(a)), and (c) equiangular radial lines through the center of the k-space (see Figure 1(d)). Note: the image intensities in (a)-(c) are scaled up so that the lower intensities in the heart region are visible, thereby causing the brighter regions outside the heart to appear white. (d), (e), and (f) show zoomed versions of images (a),(b), and (c), respectively, to clearly show the region around the heart (the region of interest).

transform data to, as well as from, the k-space domain. For this purpose, we can either (a) interpolate the non-Cartesian k-space data to a Cartesian k-space grid [24] and then rely on fast discrete-Fourier transforms to move data between the domains, or (b) form a direct functional link between the magnitude-MR data on a Cartesian grid to the non-Cartesian k-space data. In this paper, for simplicity, we use simulated k-space data (simulated from real MRI data) on Cartesian-grid-discretized radial lines. We can improve this scheme by dealing directly with radial k-space data that is not represented on a Cartesian grid using methods such as POCSENSE [25]. The key ideas in the proposed approach will, however, remain unchanged.

V. MODEL-BASED IMAGE RECONSTRUCTION

Let us denote the intensity at pixel x and time t in the reconstructed image sequence by $g(\alpha, x, t)$, which is a function of the parameter set α defined in (2). We refer to the entire sequence of reconstructed images by $g(\alpha)$. Let us denote the given sparse k-space data as $d(x, t)$. Let $F(\cdot)$ and $F^{-1}(\cdot)$ denote Fourier-transform and inverse-Fourier-transform operator, respectively. Let $W(\cdot)$ denote a *reduction* operator that zeros out those elements from the k-space where the data is not provided. Then we define an energy of the form

$$J(\alpha) = \| WFg(\alpha) - d \|_2^2, \tag{3}$$

that quantifies the discrepancy between the estimated image reconstructions and the data. In a standard inverse-methods formulation, the task is to find such image reconstructions $g(\alpha)$, i.e. such an α, that would produce k-space data as close to the given data d, thereby minimizing the energy $J(\alpha)$. That is

$$\alpha^{\text{optimal}} = \underset{\alpha}{\text{argmin}}\, J(\alpha). \tag{4}$$

We employ an iterative gradient-descent optimization strategy, with finite forward differences. Given an estimate of the parameters α^n at iteration n, we obtain

$$\alpha^{n+1} = \alpha^n - \lambda \frac{\partial J(\alpha)}{\partial \alpha} = \alpha^n - \lambda \frac{\partial J(\alpha)}{\partial g} \frac{\partial g(\alpha)}{\partial \alpha}, \tag{5}$$

where λ is the update rate. We have

$$\frac{\partial J(\alpha)}{\partial g} = 2F^{-1}(WFg(\alpha) - d). \tag{6}$$

We have found that the parameter $\beta_4(x)$ does not hold significant expressive power in the model. Thus, we can eliminate this parameter from the model and still model real data accurately using the remaining parameters. For simplicity, we also assume the phase $\phi(x)$ to be zero at all pixels in all images.

The partial derivatives of $g(\alpha)$ with respect to each of the parameters in the set α are:

$$\frac{\partial g(\alpha, x, t)}{\partial I_p(x)} = 1, \tag{7}$$

$$\frac{\partial g(\alpha, x, t)}{\partial \beta_1(x)} = C(t) * \exp\left(-\frac{t - \beta_3(x)}{\beta_2(x)}\right) H(t - \beta_3(x)). \tag{8}$$

$$\frac{\partial g(\alpha, x, t)}{\partial \beta_2(x)} = C(t) * \beta_1(x) \left(\frac{t - \beta_3(x)}{(\beta_2(x))^2}\right) \exp\left(-\frac{t - \beta_3(x)}{\beta_2(x)}\right) H(t - \beta_3(x)), \tag{9}$$

and

$$\frac{\partial g(\alpha,x,t)}{\partial \beta_3(x)} = C(t) * \beta_1(x) \left[\exp\left(-\frac{t-\beta_3(x)}{\beta_2(x)}\right)\left(\frac{H(t-\beta_3(x))}{\beta_2(x)} + \delta(t-\beta_3(x))\right)\right], \tag{10}$$

where $\delta(t)$ is the discrete delta function.

A. OBTAINING THE INPUT FUNCTION

We can derive an input function ($C(t)$) from the right-ventricular blood pool in a pre-bolus scan [26]. Only a single slice is required to estimate the input function and, hence, we can use a complete k-space acquisition. Such a pre-bolus approach has recently been used by several groups to provide accurate input functions free from saturation effects [26], [18]. The key idea here is that the input function from the right ventricle can be used with (1) to model everything in the field of view. Moreover, the input function has a good SNR because it is an average of the time-curves taken from a fairly-large spatial region.

B. OBTAINING INITIAL MODEL PARAMETERS

The model-based gradient-descent optimization process needs an initial estimate. A gradient-descent process is prone to local minima and, hence, it is reasonable that we start the model-based optimization using an initial estimate that is close to the solution. We can obtain such an initial estimate by leveraging any current state-of-the-art methods.

In this paper, we chose an inverse-method reconstruction scheme that we presented in [21] to generate the initial estimate. The initial image estimate minimizes an energy which is the sum of a fidelity term and a temporal-regularization term:

$$g^*(x,t) = \underset{g(x,t)}{\operatorname{argmin}} \parallel WFg - d \parallel_2^2 + \parallel \nabla_t g \parallel_2^2, \tag{11}$$

where ∇_t is the gradient operator along time. The second term is a penalty on the temporal gradient of the solution, and that enforces smoothness on the reconstructed time curves. This is the only prior information that we incorporate at this stage.

Using this reconstruction, we initialize $I_p^0(x)$ as the average of the first few time frames (e.g. first 3 out of a total of 30 frames), i.e.

$$\forall x : I_p^0(x) = \frac{1}{3}\sum_{t=1,2,3} g^*(x,t) \tag{12}$$

This is reasonable to do because the perfusion of the contrast agent starts only after the first few time frames and, thus, the first few images capture the same anatomical signal from the heart.

After estimating $I_p^0(x)$ in this manner, we subtract this image from all the images in the sequence and fit a parametric time-curve (using $\beta_1(x), \beta_2(x), \beta_3(x)$), independently, at each pixel x, i.e.

$$\forall x : \{\beta_1^0(x), \beta_2^0(x), \beta_3^0(x)\} = = \underset{\{\beta_1(x),\beta_2(x),\beta_3(x)\}}{\operatorname{argmin}} \parallel g(\alpha(x)) - \left[g^*(x) - I_p^0(x)\right] \parallel_2^2, \tag{13}$$

where $g(\alpha(x))$ and $g^*(x)$ denotes the respective time curves at pixel x. We use the Levenberg-Marquardt optimization scheme to find the optimal-fitting parameters. Thus,

$$\alpha^0 = \{I_p^0(x), \beta_1^0(x), \beta_2^0(x), \beta_3^0(x) : \forall x\} \tag{14}$$

forms our initial parameters estimate that we feed into the model-based optimization procedure described in Section V.

VI. OVERVIEW OF THE RECONSTRUCTION ALGORITHM

Given sparse k-space data $d(x,t)$, the proposed reconstruction algorithm proceeds as follows:

1) Obtain an initial estimate of the parameters, α^0.
   a) Use any existing method to obtain a reconstruction $g^*(x,t)$.
   b) $\forall x$: fit the model to give $\{I_p^0(x), \beta_1^0(x), \beta_2^0(x), \beta_3^0(x)\}$, as described in Section V-B.
2) Given the estimate α^n at iteration n, compute a new parameter estimate α^{n+1} via a gradient-descent scheme using finite-forward differences to minimize $J(\alpha)$.
   a) Compute $h(\alpha^n) = 2F^{-1}(WFg(\alpha^n) - d)$.
   b) $\forall x$:
   $I_p^{n+1}(x) = I_p^n(x) - \lambda_0 h(\alpha^n, x) \cdot \frac{\partial g(\alpha^n)}{\partial I_p(x)}$
   $\beta_1^{n+1}(x) = \beta_1^n(x) - \lambda_1 h(\alpha^n, x) \cdot \frac{\partial g(\alpha^n)}{\partial \beta_1(x)}$
   $\beta_2^{n+1}(x) = \beta_2^n(x) - \lambda_2 h(\alpha^n, x) \cdot \frac{\partial g(\alpha^n)}{\partial \beta_2(x)}$
   $\beta_3^{n+1}(x) = \beta_3^n(x) - \lambda_3 h(\alpha^n, x) \cdot \frac{\partial g(\alpha^n)}{\partial \beta_3(x)}$,
   where $\cdot$ denotes the dot-product operator.
3) If $\frac{\|g(\alpha^{n+1}) - g(\alpha^n)\|_2^2}{\|g(\alpha^n)\|_2^2} < \theta$, where θ is a small threshold, then terminate, otherwise go to step 2.

VII. SIMULATING CARDIAC PERFUSION DATA FROM REAL DATA

The parametric cardiac perfusion model assumes that the sequence of images is well registered and has no motion artifacts. Here we simulate well-registered data using complete-k-space data from real cardiac perfusion dynamic MR images. We apply an inverse-Fourier transform to this data, and then take the magnitude of the resulting complex number at each pixel. This essentially gives us a reconstruction using complete k-space data that does not necessarily have well-registered time frames. To enforce registration, we pixelwise fit the parametric-curve model to this magnitude data. The smoothness over the time-curves enforced by the parametric model generates fitted data that is well-registered. We use this fitted magnitude data, assuming a phase $\phi(x)$ of zero at each point, to generate simulated k-space data.

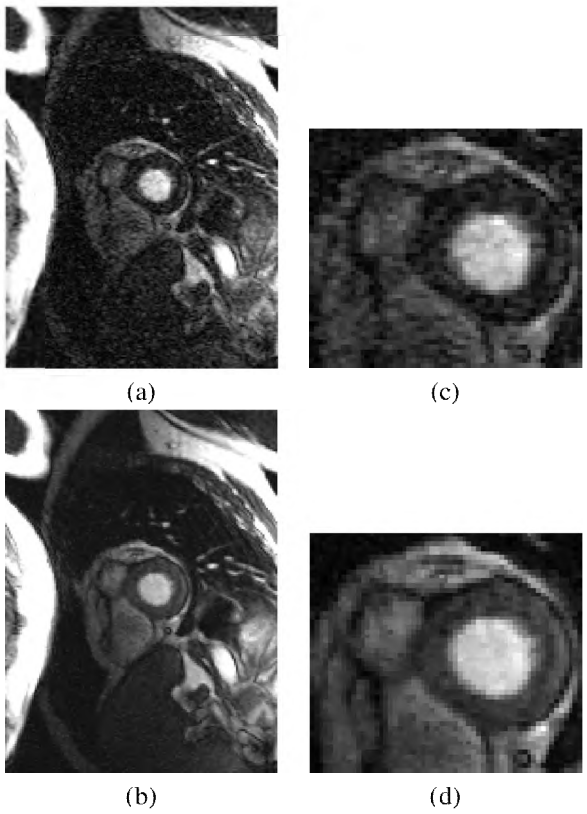

Fig. 3. Magnitude of the inverse-Fourier transforms of 100% (a) original k-space data, and (b) simulated k-space data. (c) and (d) show zoomed versions of images (a) and (b), respectively, to clearly show the region around the heart (the region of interest).

Figure 3 shows one time frame of the inverse-Fourier-transform magnitude images produced by the original (100%) data and simulated data. The simulated data closely approximates the features and variations in the original data.

VIII. RESULTS

This section gives the results of the proposed method on the simulated data comprising 29 time frames of 192 $\times$ 144 pixels each. We performed two experiments using 14% k-space data with the axis-aligned and radial sampling mechanisms described in Section IV. We chose the updates rates conservatively: $\lambda_0 = 10^{-2}, \lambda_1 = \lambda_2 = \lambda_3 = 10^{-5}$. The results are not sensitive to the specific values of these parameters. The model fitting to obtain the initial parameter estimates α^0 takes about 10 minutes for the simulated data on a standard Pentium personal computer. Each iteration of the model-based gradient-descent optimization process takes about a quarter minute and the process converges in about 50 iterations. Thus, the entire reconstruction process takes about 23 minutes for this dataset.

Figure 4 shows the reconstruction for the thirteenth time frame. Figure 4(a) and Figure 4(b) show that both sampling schemes produce visually-comparable results. However, the difference images in Figure 4(e) and Figure 4(f) show that the radial-sampling scheme produces a reconstruction with better fidelity to the original signal. The root mean square errors (RMSEs) for the two reconstructions, normalized with respect to the intensity range of the original magnitude-MR data, were 1.46% and 0.53% for the axis-aligned and radial sampling, respectively. The RMSEs for a small rectangular region around the heart (see Figure 4(c) and Figure 4(d)), normalized to the magnitude-MR intensity range in the original image in this region, were 10.18% and 1.86% for the axis-aligned and radial sampling, respectively.

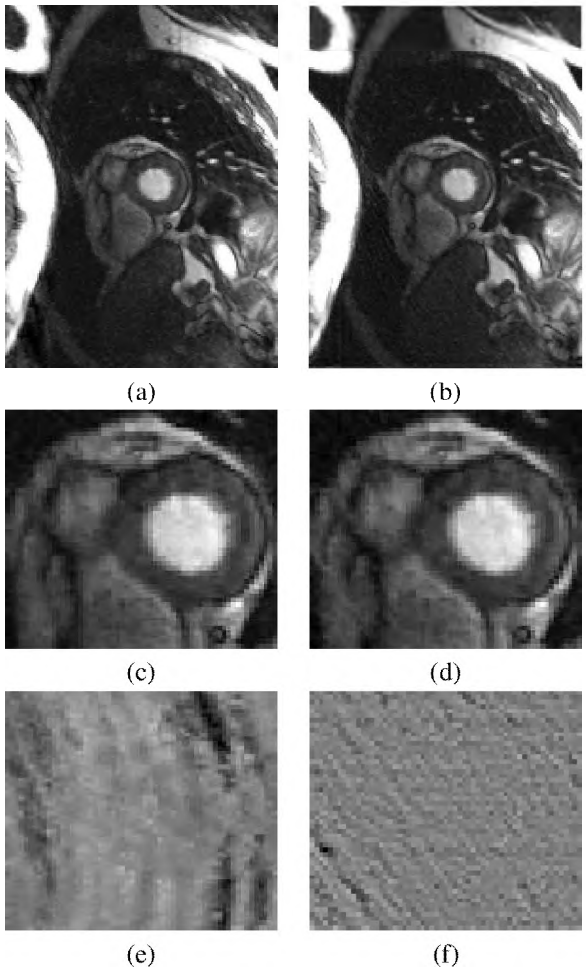

Fig. 4. One time frame among the reconstructed magnitude-MR sequence for 14% k-space data acquired using the (a) axis-aligned sampling strategy (see Figure 1(a)), and (b) radial sampling strategy (see Figure 1(b)). (c) and (d) show zoomed versions of images (a) and (b), respectively, to clearly show the region around the heart (the region of interest). (e) and (f) show the difference images for the regions around the heart between the simulated data (ground truth) and the reconstructions in (a) and (b), respectively.

IX. DISCUSSION AND CONCLUSIONS

The proposed reconstruction method is more computationally intensive than many of the methods in current use. While some low resolution rapidly reconstructed images are important to gauge the immediate success of the acquisition, an off-line reconstruction taking thirty minutes or even an hour is acceptable to make a diagnosis—post-processing required approximately an hour per scan in a recent clinical study of 102 subjects using SENSE [1].

As well, the proposed algorithm is trivially parallelizable.

The implementation can be multi-threaded to exploit multi-processor computer architectures, such as those common in dual-processor PCs, to yield virtually linear speedup.

This model assumes that the sequence of images is well registered with no motion artifacts. We can incorporate registration into the proposed reconstruction scheme so that in-plane translations are estimated, along with the images, at each time frame. Alternatively, motion can, in theory, be tracked with a navigator or respiratory strap and incorporated into the reconstruction. These issues are beyond the scope of the current work, which is to establish the potential of a model-based reconstruction method for dynamic MRI.

The model-based reconstruction approach was shown to perform well with simulated data. The simulations were generated from acquired magnitude data. Thus, the k-space data possessed Hermitian symmetry. An important part of future work comprises more experiments that explicitly obtain a pre-contrast phase map and then estimate the image phase temporal variations (which are small). It will be important to assess how well the proposed method works in practice.

The proposed method makes no assumptions regarding the aliasing of the data and, hence, the method can use arbitrary sampling patterns. This also means that the method can incorporate some ideas, from kt-BLAST-type techniques [28], of estimating the overlaps due to a specific sampling pattern. The proposed method can also be combined with multi-coil methods. The multi-coil methods exact an SNR penalty, while the model-based reconstruction improves SNR.

ACKNOWLEDGEMENT

This work received support from the NSF EIA0313268 grant.

REFERENCES

[1] S. Plein, A. Radjenovic, J. P. Ridgway, D. Barmby, J. P. Greenwood, S. G. Ball, and M. U. Sivananthan, "Coronary artery disease: myocardial perfusion MR imaging with sensitivity encoding versus conventional angiography," Radiology, vol. 235, pp. 423-30, 2005.

[2] J. Schwitter, D. Nanz, S. Kneifel, K. Bertschinger, M. Buchi, P. R. Knusel, B. Marincek, T. F. Luscher, and G. K. v. Schulthess, "Assessment of myocardial perfusion in coronary artery disease by magnetic resonance. A comparison with positron emission tomography and coronary angiography," Circ, vol. 103, pp. 2230-2235, 2001.

[3] N. M. Wilke, M. Jerosch-Herold, A. Zenovich, and A. E. Stillman, "Magnetic Resonance first-pass myocardial perfusion imaging: clinical validation and future applications," J. Magn. Reson. Imaging, vol. 10, pp. 676-685, 1999.

[4] H. Thiele, S. Plein, J. P. Ridgway, and A. others, "Effects of missing dynamic images on myocardial perfusion reserve index calculation: comparison between an every heartbeat and an alternate heartbeat acquisition," J Card Magn Reson, vol. 5, pp. 343-352, 2003.

[5] F. A. Breuer, P. Kellman, M. A. Griswold, and P. M. Jakob, "Dynamic autocalibrated parallel imaging using temporal GRAPPA (TGRAPPA)," Magn Reson Med, vol. 53, pp. 981-5, 2005.

[6] P. Kellman, F. H. Epstein, and E. R. McVeigh, "Adaptive sensitivity encoding incorporating temporal filtering (TSENSE)," Magn Reson Med, vol. 45, pp. 846-852, 2001.

[7] J. A. Darcy, D. J. Collins, I. J. Rowland, A. R. Padhani, and M. O. Leach, "Applications of sliding window reconstruction with cartesian sampling for dynamic contrast-enhanced MRI," NMR in Biomedicine, vol. 15, pp. 174-183, 2002.

[8] A. L. Alexander, Y. J. Wu, and E. V. R. Di Bella, "Improved dynamic image consistency with k-space interpolation in time (K-SPINIT)," presented at Int Soc Magn Reson Med, pp., Honolulu, 2002.

[9] A. C. Larson and O. P. Simonetti, "Real-time cardiac cine imaging with SPIDER: steady-state projection imaging with dynamic echo-train readout," Magn Reson Med, vol. 46, pp. 1059-66, 2001.

[10] D. T. Boll, E. M. Merkle, D. M. Seaman, R. C. Gilkeson, A. P. Larson, O. P. Simonetti, J. L. Duerk, and J. S. Lewin, "Comparison of ECG-gated rectilinear vs. real-time radial K-space sampling schemes in cine True-FISP cardiac MRI," J Cardiovasc Magn Reson, vol. 6, pp. 793-802, 2004.

[11] F. R. Korosec, R. Frayne, T. M. Grist, and C. A. Mistretta, "Time-resolved contrast-enhanced 3D MR angiography," Magn Reson Med, vol. 36, pp. 345-51, 1996.

[12] J. Du, T. J. Carroll, H. J. Wagner, K. Vigen, S. B. Fain, W. F. Block, F. R. Korosec, T. M. Grist, and C. A. Mistretta, "Time-resolved, undersampled projection reconstruction imaging for high-resolution CE-MRA of the distal runoff vessels," Magn Reson Med, vol. 48, pp. 516-22, 2002.

[13] M. Doyle, E. G. Walsh, R. E. Foster, and G. M. Pohost, "Rapid cardiac imaging with turbo BRISK," Magn Reson Med, vol. 37, pp. 410-7, 1997.

[14] B. Madore, G. H. Glover, and N. J. Pelc, "Unaliasing by Fourier-encoding the overlaps using the temporal dimension (UNFOLD), applied to cardiac imaging and fMRI," Mag Reson Med, vol. 42, pp. 813-828, 1999.

[15] W. G. Rehwald, R. J. Kim, O. P. Simonetti, G. Laub, and R. M. Judd, "Theory of high-speed MR imaging of the human heart with the selective line acquisition mode," Radiology, vol. 220, pp. 540-547, 2001.

[16] D. C. Peters, D. B. Ennis, and E. R. McVeigh, "High-resolution MRI of cardiac function with projection reconstruction and steady-state free precession," Magn Reson Med, vol. 48, pp. 82-8, 2002.

[17] E. V. R. DiBella, Y. J. Wu, A. L. Alexander, D. L. Parker, D. Green, and C. J. McGann, " Comparison of temporal filtering methods for dynamic contrast MRI myocardial perfusion studies," Magn Reson Med, vol. 49, pp. 895-902, 2003.

[18] T. F. Christian, D. W. Rettmann, A. H. Aletras, S. L. Liao, J. L. Taylor, R. S. Balaban, and A. E. Arai, "Absolute myocardial perfusion in canines measured by using dual-bolus first-pass MR imaging," Radiology, vol. 232, pp. 677-84, 2004.

[19] B. P. Sutton, D. C. Noll, J. A. Fessler. Fast, iterative, field-corrected image reconstruction for MRI. IEEE Tr. Med. Im., 22(2):178-188, 2003.

[20] Noll, D.C. and J.A. Fessler and B.P. Sutton. Conjugate phase MRI reconstruction with spatially variant sample density correction. IEEE Tr. Med. Im., 24(3):325-336, 2005.

[21] O. Portniaguine, C. Bonifasi, E. V. R. DiBella, and R. Whitaker, "Inverse methods for reduced k-space acquisition," presented at ISMRM, pp. 481, Toronto, Canada, 2003.

[22] D. C. Peters, F. R. Korosec, T. M. Grist, W. F. Block, J. E. Holden, K. K. Vigen, and C. A. Mistretta, "Undersampled projection reconstruction applied to MR angiography," Magn Reson Med, vol. 43, pp. 91-101, 2000.

[23] K. Scheffler and J. Hennig, "Reduced circular field-of-view imaging," Magn Reson Med, vol. 40, pp. 474-80, 1998.

[24] H. Moriguchi and J. L. Duerk, "Iterative Next-Neighbor Regridding (INNG): improved reconstruction from nonuniformly sampled k-space data using rescaled matrices," Magn Reson Med, vol. 51, pp. 343-52, 2004.

[25] A. A. Samsonov, E. G. Kholmovski, D. L. Parker, and C. R. Johnson, "POCSENSE: POCS-based reconstruction for sensitivity encoded magnetic resonance imaging," Magn Reson Med, vol. 52, pp. 1397-406, 2004.

[26] H. Kostler, C. Ritter, M. Lipp, M. Beer, D. Hahn, and J. Sandstede, "Prebolus quantitative MR heart perfusion imaging," Magn Reson Med, vol. 52, pp. 296-9, 2004.

[27] Matteo Frigo and Steven G. Johnson, "The Design and Implementation of FFTW3," Proceedings of the IEEE 93 (2), 216.231 (2005). Invited paper, Special Issue on Program Generation, Optimization, and Platform Adaptation. http://www.fftw.org

[28] A. Samsonov, E. V. R. DiBella, P. Kellman, and E. G. Kholmovski, "Adaptive K-T BLAST/K-T SENSE for accelerating cardiac perfusion MRI," presented at Soc Cardiovasc Mag Reson, pp. 277-278, San Francisco, 2005.